Discussion on backarc mantle melting in the central Andean subduction zone, based on results of magnetotelluric studies

D. Eydam* & H. Brasse
Free University of Berlin, Malteserstr. 74-100, 12249 Berlin

Abstract

Long-period magnetotelluric measurements in the Bolivian orocline revealed a large conductor in the backarc upper mantle of the central Andean subduction zone at 18°S. Data analysis and interpretation by 2-D inversion has already been described by Brasse & Eydam (2008a) who interpreted this conductor as an image of partial melt triggered by fluid influx from the subducting slab.

Remarkable are its high conductivities ranging up to above 1 S/m and implying high melting rates of more than 6vol%. However, regarding the distribution of intermediate depths seismicity which marks dehydration reactions in the subducting slab, one has to note the large distance of more than 60 km between fluid source and the assumed fluid-triggered partial melting of mantle peridotite. How do actual concepts of subduction zone dynamics fit to this resistivity image?

There are at least two approaches which are both followed by in the subsequent discussion: first is to study the mobility of deep fluids in subduction zones, second is to study the mobility of the slab itself.

Introduction

Ocean-continent subduction zones are earth regions of major raw material recyclings. Hot magmas erupt nearby where cold oceanic lithosphere subducts. This apparently contradictory observation is explainable by consumption of deep slab-derived fluids for flux melting of the peridotitic mantle in the asthenospheric wedge:

Hydrous minerals in the oceanic lithosphere are progressively dehydrating during subduction. The hereby released water may trigger partial melting of the overlying asthenospheric wedge by lowering mantle solidus generally at depths below 80 km. Melts and fluids ascent with some intermediate storage at density contrasts at the Moho or intra-crustal boundaries and give rise to arc and backarc volcanism. Due to their

*now at GFZ Potsdam, Telegraphenberg, 14437 Potsdam

enhanced conductivities, saline fluids and (hydrous) melt should principally be detectable by deep electromagnetic sounding methods, as was demonstrated, e.g., in the Cascadia/Juan de Fuca subduction zones (Kurtz *et al.*, 1986; Wannamaker *et al.*, 1989; Varentsov *et al.*, 1996).

Hydrous phases in the oceanic crust relevant for sub-arc water release are amphibole and lawsonite. Amphibole is abundant in the basaltic oceanic crust and decays only slightly pressure-dependent at 65-80 km depths, marking the transition from blueschist to eclogite facies. In contrast, lawsonite can be stable up to high pressures of 8.4 GPa ($z \approx 250$ km) and dehydrates when temperatures exceed 700-800°C. Mantle water release is mainly controlled by serpentinite dehydration between 500-700°C. Serpentinite can be stable up to high pressures of 6 GPa where it transforms through a water-conserving reaction to the hydrous DHMS (*Dense Hydrous Magnesium Silicat*) -phase A.

The amount of released water thus strongly depends on the thermal structure as well as on subduction geometry. Young and slowly subducting slabs may dehydrate completely whereas old and rapidly subducting lithospheres may import large amounts of mantle water into the deeper mantle, making them crucial for the global water cycle.

The definitive amount of deep fluids in subduction zones is still uncertain because of the dependency of dehydrations from slab heating via mantle convection which in turn, strongly depends on water content in the wedge, besides other mostly poorly constrained parameters.

Geological setting

The central Andean subduction zone

Along 7000 km length the oceanic Nazca plate subducts beneath the South American continental margin where the Andes evolved as a Neogene volcanic chain embedded in a compressive backarc tectonic setting. Holocene volcanism is seperated in four active segments, the austral, southern, central and northern volcanic zone (fig. 1).

Characteristic for the whole subduction system are low slab dips of less than 30° and inactive volcanism in regions where aseismic ridges subduct. Those hot oceanic lithospheres probably flatten at main depths of sub-arc water release due to a retard of dehydration and thus density increase of the slab which may lead to 'horizontal subduction' over several hundreds of kilometres (Gutscher *et al.*, 2000). Therefore, slab pull and buoyancy forces should be quite equilibrated probably making the slab mobile in geological time scales.

The Bolivian orocline (13-28°S) encompasses the central volcanic zone (CVZ) where the oldest part of the Nazca plate (55 Ma) subducts obliquely with an angle of N77°E and with a current velocity of 6.5 cm/a (Klotz *et al.*, 2006). Convergence rate has continuously slowed down from high 15 cm/a since the breakup of the oceanic Farallon plate in Nazca and Cocos plate 26 Ma ago (Somoza, 1998).

During the highly compressive Miocene regime, stresses are mainly relaxed by extreme

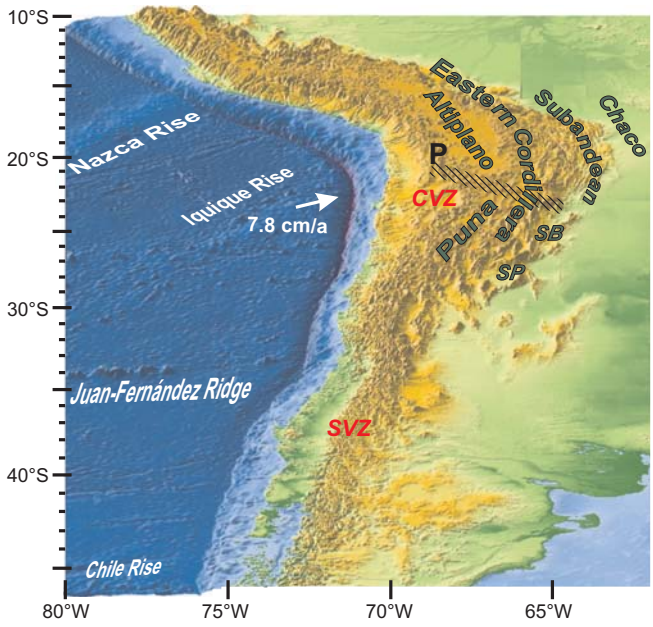

Figure 1: South American subduction zone with structural units of the central volcanic zone (CVZ) backarc and foreland. Hachures: Altiplano-Puna transition between 22-24°S; SB, SP - thick-skinned folding and thrusting in the Santa-Bárbara system and Sierras Pampeanas; P - Pica-Gap of Holocene volcanism (19.2-20.7°S) where Iquique Rise subducts (Wörner *et al.*, 2000); SVZ - southern volcanic zone. Convergence rate after Somoza (1998).

crustal shortening, thickening and uplift of the entire Andean arc and backarc region (e.g., Allmendinger *et al.*, 1997; Scheuber *et al.*, 1994; Elger *et al.*, 2005). As a consequence the Altiplano-Puna high plateau developed, encompassing the highest volcanoes of the world (e.g., 6500 m for Sajama volcano) in the Western Cordillera to the west, rough mountain ranges in the Eastern Cordillera at the eastern boundary and the intramontanous drained Altiplano and Puna basins with thick Miocene stratas in-between.

The up to 1800 km long and 350 km wide Altiplano-Puna plateau is the worldwide greatest high plateau in a subduction context. Crustal thickness is enormous (up to 75 km; e.g., Wigger *et al.*, 1994) and decreases beyond the plateau extension to normal values for continental lithosphere of 35-40 km. Likewise volcanism in the CVZ is highly crustally contaminated against more island-arc denoted lavas in the SVZ.

Altiplano and Puna form an unique tectonomorphic entity within the orogen although their morphology differs. While the Altiplano in the north is rather flat and tectonically quiet, the Puna in the south is pervaded by many deep reaching, active horst- and graben structures. Average elevations are around 3700 m in the Altiplano and 4500 m in the Puna.

Actual compressive tectonics are mainly restricted to the Andean foreland, where westvergent thin-skinned thrusting in the Subandean to the north change to thick-skinned thrusting in the Santa Bárbara system and Sierras Pampeanas to the south (Allmendinger *et al.*, 1997). At Altiplano latitudes, the comparatively fast westward subduction of the Brazilian Shield enhances the compressive backarc regime.

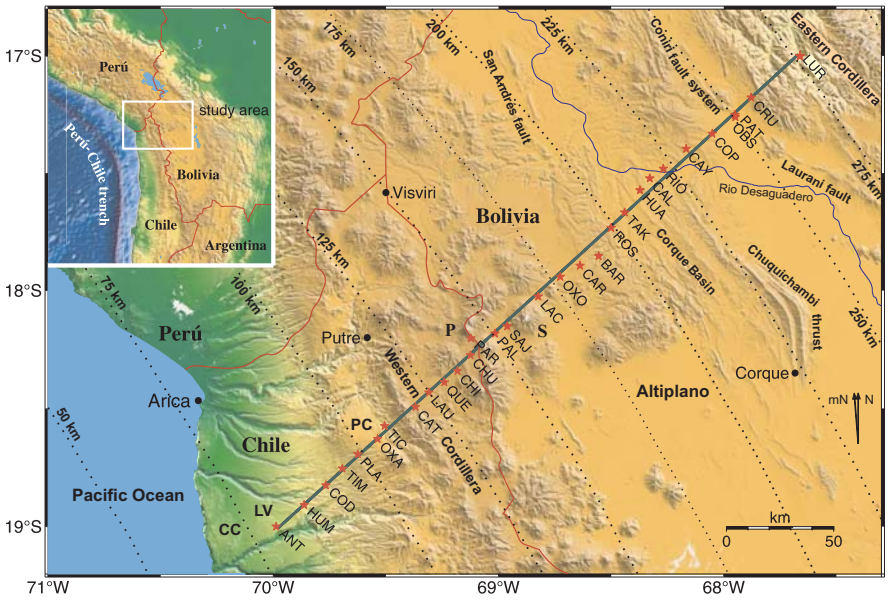

Figure 2: Survey area with locations of the 30 MT sites in the Bolivian orocline. Profile trends roughly perpendicular to the strike of main morphological units and to the contour lines of the Wadati-Benioff zone (dotted lines). CC denotes Coastal Cordillera, LV Longitudinal Valley and PC Precordillera; P, S are Parinacota, Sajama volcanoes; mN is magnetic north.

The survey area

The magnetotelluric profile transverses the central Bolivian orocline from the Coastal Cordillera in northermost Chile, to the active volcanic arc and the Altiplano in central Bolivia and ends in the Eastern Cordillera. The profile follows a general trend of N48°S which is roughly perpendicular to main structural units as well as to contour lines of the Wadati-Benioff zone (fig. 2).

Main morphological units in the forearc are paralleling the trench and correspond to an ancient magmatic arc which shifted eastward through time, recordable since the Jurassic in the Coastal Cordillera, afterwards in the Longitudinal Valley, in the Precordillera and until the Neogene in the Western Cordillera (Scheuber *et al.*, 1994). The exposure of the forearc crust to periods of extensive and long-lived magmatism gave rise to the formation of deep, long and wide fault zones (sub-)paralleling the trench among which some are still active like the Precordillera Fault System at 19.2-21°S. Here, large copper deposits evidence strong fluid circulation and mineralisation after the eastward shift of the arc 32 Ma ago.

In the closer survey area, the forearc is incised by deep, E-W running valleys which open to the ocean and may have served as Miocene drainage systems. Some of them may be associated with active faults (Wörner *et al.*, 2000). A system of west vergent, steeply dipping thrust faults in the eastern Precordillera, the West-Vergent-Thrust-System, marks the transition to the high plateau and is thought to be the location of major plateau uplift (Muñoz & Charrier, 1996).

The smooth monoclinal western slope of the high plateau is locally shaped by huge land slides, e.g., the Oxaya collaps 12 Ma ago (Wörner *et al.*, 2002). In the West-

ern Cordillera, Plio-Pleistocene to recent, andesitic to rhyodacitic stratovolcanoes are build on thick layers of ignimbrites which are widespread throughout the entire forearc and are dated between 22-19 Ma (Oxaya Ignimbrites) and to 2.7 Ma (Lauca-Pérez Ignimbrite) (Wörner *et al.*, 2000).

The Altiplano can be separated into the volcanic Mauri region to the west and in huge sedimentary basins easterly. The San-Andrés fault marks the boundary in-between and limits the Arequipa terrane to the east, a component of the Arequipa-Antofalla massif which comprises up to 2 Ga old rocks and underpins the volcanic arc probably along the whole plateau (see in James & Sacks, 1999). The most prominent feature in the Altiplano is the 80 km wide Corque basin, a deep asymmetric sedimentary basin with thick and folded tertiary strata, exceeding 10 km thickness (Hérail *et al.*, 1997) and evidencing orogeny dynamics during Miocene's pronounced compressive regime.

To the east the basin is controlled by the Chuquichambi thrust system. The Coniri-Laurani fault system marks the transition to the Eastern Cordillera, the rough eastern flank of the plateau. Farther to the east the Interandean Zone and Main Andean Thrust separate the Altiplano plateau from the actual deformation front in the Subandean, with thin-skinned folding and thrusting holding the record of shortening rates within the study area (Allmendinger *et al.*, 1997).

After the Oligocene eastward shift of the magmatic arc, Neogene volcanism first relived in the Eastern Cordillera 27 Ma ago and afterwards encompassed the whole plateau region. Neogene volcanism of the Altiplano plateau is composed of three main units: Pliocene to recent stratovolcanoes are erupting in the main arc and Miocene to recent backarc calderas and mafic mongenetic pulses are distributed in the arc and backarc.

Intensive ignimbritic volcanism erupted 10-4 Ma ago at the Altiplano-Puna transition between 21-24°S and formed one of the greatest ignimbrite provinces of the earth, the Altiplano-Puna-Volcanic-Complex. Recent ignimbrite eruptions are older than 1 Ma. The high water, phenocrystal and silicate content signify long storage in huge crustal magma chambers with pronounced fluidal circulation.

Holocene volcanic activity is less than in the Puna where the lithosphere probably is 50 km thinner (Whitman *et al.*, 1996). Volcanism in the closer survey area is categorised from dormant (Parinacota) to solfataras state with intensive fumarolic activity at Guallatiri volcano. The profile volcano Parinacota may possess a stable magma chamber with only minor magmatic input.

Glance on data analysis and 2-D inversion

We measured horizontal components of the electromagnetic field as well as the vertical magnetic field for long periods between 10 and 20 000 s. Data analysis and its interpretation by 2-D inversion has already been described by Brasse & Eydam (2008a) and will not be replicated in this article.

Some important results are just mentioned: We could not resolve subduction-related features near the slab, like fluid curtains or fluid and melt pathways, due to significant

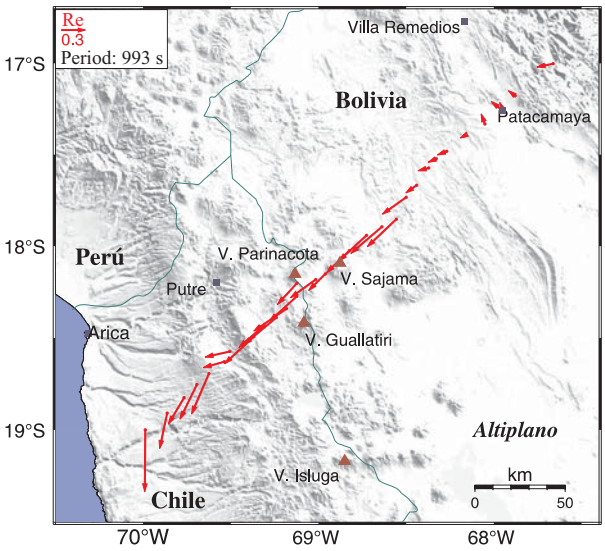

Figure 3: Real part induction arrows in Wiese convention for one chosen period demonstrating the remarkable good alignement of arrows in profile direction. Arrows in the forearc are deflected; they are pointing parallel to the coast.

3-D effects in the forearc. This can easily be seen in the behavior of real part induction arrows pointing parallel to the coast (fig. 3) which is also observed in other coastal regions in Chile so that one might call them 'Chile arrows'. Brasse *et al.* (2008b) showed that they can be explained by anisotropy in the forearc crust. Seven forearc station data were thus discarded from further interpretation by 2-D inversion.

Induction arrows as well as the analysis of impedance data, which reveals phase-sensitive skew values below 0.3 for plateau sites, suggest fairly good electrical 2-D approximation for the plateau region. We observe a remarkable good alignement of middle to long period real part induction arrows in profile direction, as seen in figure 3. Correspondingly, electrical strike derived by impedance data is fairly perpendicular to the profile. Real arrows disappear in the central Altiplano where resistivities are signifcantly reduced for all sites and rotation angles and follow a well marked downward trend for longer periods indicating assumably well conducting features at greater depths.

2-D inversions were performed with the inversion program of Rodi & Mackie (2001). Accounting for the consistency of induction arrows in the Altiplano, tipper weight was set high by assigning a small (absolute) error floor of 0.02. Error floors for resistivities and phases were set to 20% and 5% in order to overcome the static shift problem. Reliable models are achieved after numerous experiments inculding tests of starting models, specifying the regularisation term and further resolution tests (see Eydam, 2008).

Discussion on backarc mantle melting

The final model, shown in figure 4, is obtained by jointly inverting tippers, TE and TM mode apparent resistivities and phases. Static effects were accounted for by using the program internal adjustment. Fair regularisation parameters lie around 20. Model RMS is 1.80, with larger misfits at the electrically less 2-D plateau borders (see Brasse & Eydam, 2008a).

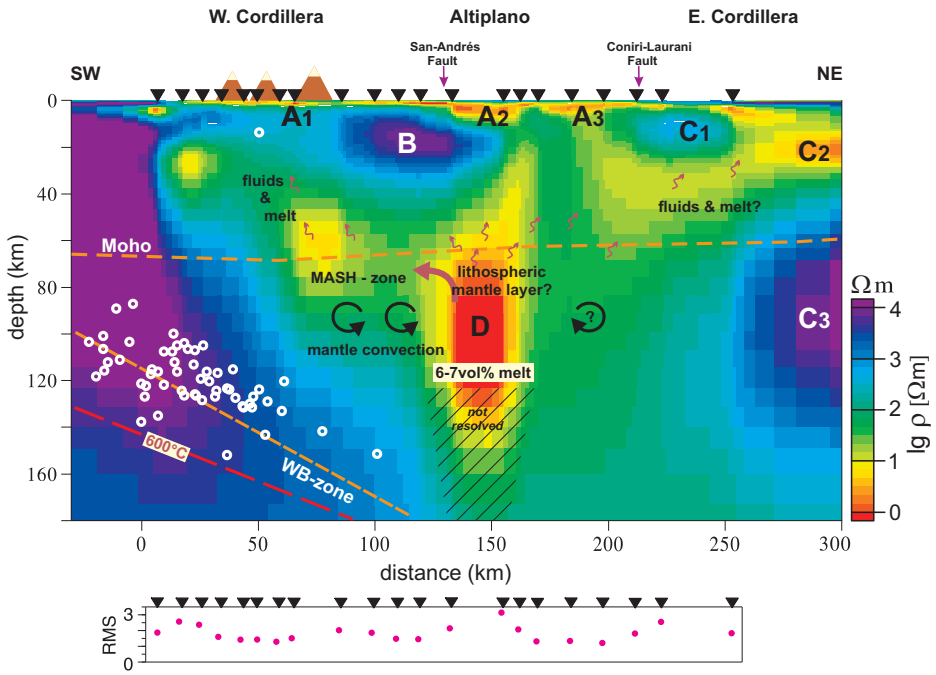

Figure 4: Final resistivity model with suspectable fluid & melt dynamics - Ai: Corque and minor basins, B: Arequipa block(?), Ci: structures beneath the Eastern Cordillera, D: backarc mantle magma reservoir plus rise of fluids and melts. Circles indicate location of mayor earthquakes (M > 4.5, Engdahl & Villaseñor, 2002). WB denotes Wadati-Benioff zone. MASH-zone stands for melting, assimilation, storage and homogenisation zone of arc magmas. Below: RMS for the inverted station data.

The large upper mantle conductor D is interpreted as an image of partial melts triggered by fluid influx from the slab. Conductivities range up to above 1 S/m and are definitely required by data down to 115 km depth, particularly to fit the downward trends in long period app. resistivities; they are consistent with data down to slab depths. This implies high melting rates of more than 6vol% (Eydam, 2008).

Lithospheric mantle material should stabilise magma and trap hot fluids which otherwise would rapidly trigger wide scale crustal melting like this is the case in the southern Altiplano (e.g., ANCORP Working Group, 2003). This is consistent with seismic data from Dorbath & Granet (1996) who resolve lithospheric characteristics just beneath the Altiplano Moho.

The source region of subduction related magmatism is offset from the arc by almost 100 km, implying fluid and melt storage near the Moho (in so called MASH-zones) and non-vertical rise of only few fluidal and molten material towards the volcanoes. This accords to low volcanic productivity in the closer survey area, while lavas are bearing highly modified mantle signatures (Wörner *et al.*, 1992). Magma and fluid lateral motion should be enforced by internal convections.

This 'scenario' implies a widely hydrated crust and upper mantle beneath the high plateau which is consistent with other geophysical anomalies, like high heat flow densities (e.g., Springer & Förster, 1998), neagtive Bouguer anomalies (Tassara *et al.*, 2006), slow seismic velocities in a thick and highly absorbing crust (e.g., Beck & Zandt, 2002)

	water import	water release in 80-180 km depth			
component of oceanic plate	per m^2 Nazca plate [kg]	in percentage of imported water	per subducted meter [kg]	per Ma [10^6 kg][2)]	in neogene cycle[3)] WC = VA [10^6 kg]
sediments	1 700	20	340	32	832
crust	170 000	55	93 500	8 883	230 958
mantle	250 000[1)] 1 000 000[2)]	60	150 000[1)] 600 000[2)]	14 250[1)] 57 000[2)]	370 500[1)] 1 482 000[2)]
total	421 700 1 171 700		243 840 693 840	23 165 65 915	602 290 1 713 790

Table 1: Water budget for main dehydration depths in the central Andean subduction zone calculated by using 1) a standardised mantle hydration model after Rüpke *et al.* (2004), 2) a mantle hydration model deduced from local data after Ranero & Sallarès (2004) and 3) by using averaged subduction rates after Somoza (1998). WC - Western Cordillera, VA - main volcanic arc.

and a strong mantle signature of geothermal fluids (Hoke *et al.*, 1994).

Estimation of arc and backarc water release

A critical mind might state that the ability of water import is probably not sufficient to nurture such wide scale melting of mantle material. Table 1 shows the water balance for slab dewatering at main dehydration depths between 80-180 km, deduced from intermediate depths microseismicity published in David (2007) and seen in figure 7.

For the calculation we used hydration estimates after Rüpke *et al.* (2004) modified by local data (fig. 5). Mantle hydration is poorly definable and depends on depth and density of bending related faults as well as on the thermal structure of the oceanic lithosphere. Therefore estimates based on regional seismic and gravimetric data evaluated by Ranero & Sallarès (2004) are four times higher than those assumed by Rüpke *et al.* (2004) who standardised hydration levels with regards to the age of the lithosphere. Water balances are presented for both models.

The presented water releases are based on results of chemo-thermo-mechanical modellings performed by Rüpke *et al.* (2004) who solved for slab dehydration during sub-

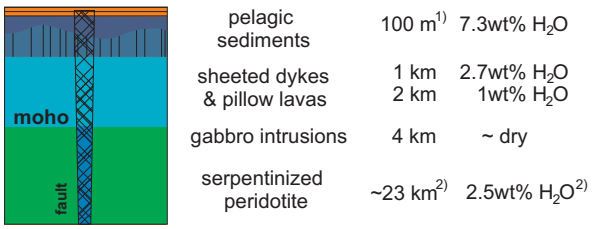

Figure 5: Oceanic lithosphere with estimated water content in sediments, crust and mantle after Rüpke *et al.* (2004) modified by local data: 1) the thickness of sedimentary deposits after von Huene *et al.* (1999) and 2) mantle hydration after Ranero & Sallarès (2004).

duction regarding latent heat consumption and neglecting shear heating[1] (fig. 6).

Thereafter, one column of one square metre Nazca lithosphere releases 700 t water at main dehydration depths (80-180 km) which sums up to 1.7 Gt water regarding the entire Neogene cycle of Nazca plate subduction starting 26 Ma ago (Sempere *et al.*, 1990). Using the molar volume of water at 120 km depths, this mass fills a cross-section of more than 1500 km^2 which finally lies in the dimension of the mantle magma reservoir.

Phases of oroclinal bending might have been important for the water budget, because bending related faults should have opened parallel as well as perpendicular to the trench so that large amounts of water could have been fixed in the mantle.

Slab-derived water in the mantle wedge should thus be sufficient to trigger a wide scale melting of mantle material, well noticing the presumably prior hydration of the Western Cordillera as pre-Neogene backarc. If the residual water, retained in the oceanic lithosphere, is released as well, the cross-section will expand for additional 170 km^2 in case of complete crustal dehydration resp. 880 km^2 for complete mantle dehydration which points out the role of oceanic mantle for subduction zone dynamics.

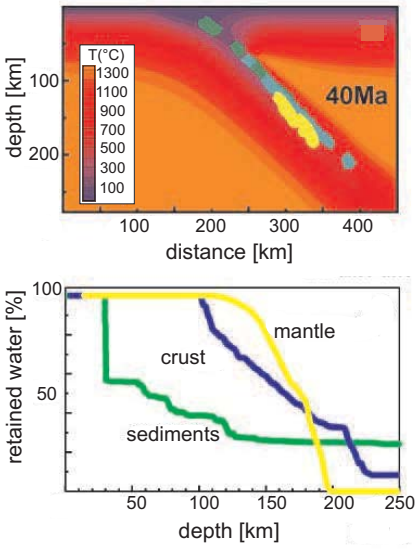

Figure 6: Dehydration of oceanic lithosphere during subduction, presented above) as main depths' water release of sediments, crust and mantle and below) as percentage of retained water respectively; after Rüpke *et al.* (2004).

The double seismic layer shown in figure 7 allows allocating the events to stability limits of mayor hydrous minerals in the oceanic lithosphere which can be used to predict slab temperatures at depths.

Crustal seismicity stops around 140 km depth, whereas seismicity in the oceanic mantle is ongoing until the stability limit of serpentine in 180 km. Lawsonite is the only hydrous mineral in the crust which is stable down to 140 km depth. Lawsonite decay starts at the hot interplate boundary at shallower dephts and proceeds during subduction to deeper slab layers where temperatures at 140 km depth should exceed 730°C. Serpentine as the main hydrous mantle phase should still be present at 180 km depth where it transforms through a water-conserving reaction to mantle phase A (Eydam, 2008).

These estimates correspond to a fairly warm subduction system although the Nazca plate is quite old (55 Ma). Shear heating at the interplate boundary may elevate temperatures in the oceanic crust, because lubricates like sediments are sparse in the

[1]Modifying the mantle hydration model to higher estimates after Ranero & Sallarès (2004) will change the modelling results to even larger water releases than calculated in table 1, considering that dehydrations are mostly exothermic reactions.

central Andean subduction zone as a consequence of its arid climate (Lamb & Davis, 2003). Thus more water than listed in table 1 may be released into the mantle wedge.

Dehydrations finish below 200 km depth, suggesting that slab-derived fluids supply partial melting of mantle peridotite more than 60 km laterally away from their source region. Might this be possible?

Discussion on fluid mobility

There are several models describing fluid mobility in subduction zones like fluid channeling along cracks opened by dehydration induced hydrofracturing, lateral transports in the coupled mantle wedge, porous flows and thermally induced convections in the asthenospheric wedge.

At considered depths hydrofractured faults shouldn't reach far into the mantle and a coupled mantle wegde should be unrealistically thick to explain the requested transportation lengths. Porous flows start when interstitial fluids or melts interconnect depending on temperature, fluid salinity and melt viscosity. Deep slab-derived fluids are highly saline (Scambelluri & Philippot, 2001) and temperatures below 140 km depth definitively exceed 620°C (see above), the minimum temperature of pure water interconnection in an olivine matrix (Mibe *et al.*, 1999).

Water enhances mantle convection via lowering the peridotitic solidus in the mantle wedge. This effect may be more pronounced than expected so far, considering the very slow reaction kinetics of olivine melting in laboratory experiments (Grove *et al.*, 2006). The correction of peridotitic solidus to much lower temperatures, e.g. to 860°C at 100 km depth, implies that first water-enriched melts may be generated just above the slab. The melt fraction should be minor due to fast segregation of the low-viscous melts into lower and hotter mantle regions.

Additionally, water import in the central Bolivian orocline might have been temporarily elevated in phases of its oroclinal bending leading to a significant reduction of mantle viscosity and enabling effective material transports via thermal convections, like it is modelled for some general case studies by Gerya *et al.* (2006). Saline fluids and melts may be transported far into the hotter backarc mantle where melt fractions rise and segregation rates decrease and fluids and melts become detectable by magnetotellurics.

Models of mantle convection deal with numerous low constrainted parameters, like the degree of mantle hydration, shear heating at the interplate boundary, latent heat produced by mineral reactions or advective heat transports by fluids and melts. Therefore mantle rheology is only poorly definable and viscosity values may differ over several magnitudes.

Water release at intermediate depths plays thus an important role in subduction zone dynamics. Currie & Hyndman (2006) even postulate that hot backarc mantles are a fundamental characteristic of an ocean-continent subduction zone. And indeed, other magnetotelluric images from the central Andean backarc mantle seem to concur with this: Schwarz & Krüger (1997) modelled 0.02 S/m conductive mantle features at the

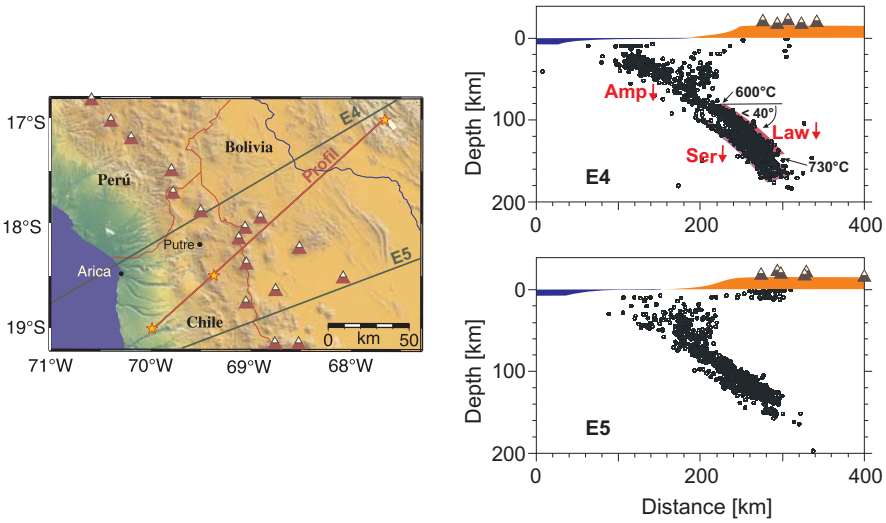

Figure 7: Local microseismic events (M > 1) after David (2007) with map of projection lines E4, E5 and MT profile. Above: Events allocated to decay temperatures of hydrous minerals, this are in the crust: Amp - amphibole and Law - lawsonite and in the oceanic mantle: Ser - serpentine. Note the double seismic layer.

transition to the Puna around 23°S and northwards at 20-21°S upper mantle material seems to be quite conductive as well with values over 0.05 S/m (Lezaeta, 2001), though electromagnetic fields are severely attenuated by a crustal high conductivity zone here (Brasse *et al.*, 2002).

Discussion on the mobility of the slab itself

The Nazca plate subducts along the whole margin with small dip angles between 25-30° or even horizontally in greater depths at some segments (so called 'flat subduction') where volcanism above is inactive.

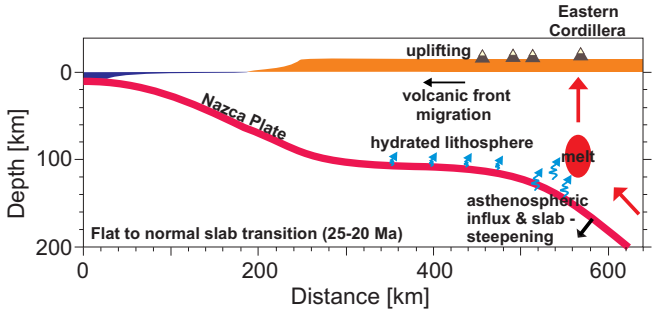

Figure 8: 'Mobile slab model' for the central Andes after James & Sacks (1999). Due to retarded dehydration at intermediate depths, slab flattens and dewaters sparsely, insufficient to melt but to hydrate the base of the overlying lithosphere. Slab compacts and steepens again when hot asthenospheric material influx and triggers effective dehydrations; magmatism and volcanism above develop.

Thus, slab pull and buoyancy forces are fairly equilibrated and the slab may react sensible to density changes due to retarded dehydrations; it gets mobile in geological time scales.

Such 'chemically controlled slab mobility' was already discussed by James & Sacks (1999) and applied on central Andean history by supposing a period of flat subduction 35-25 Ma ago, basically due to absent lava dates for this period (fig. 8).

Remarkable is the slight slab steepening in the central orocline (fig. 7).

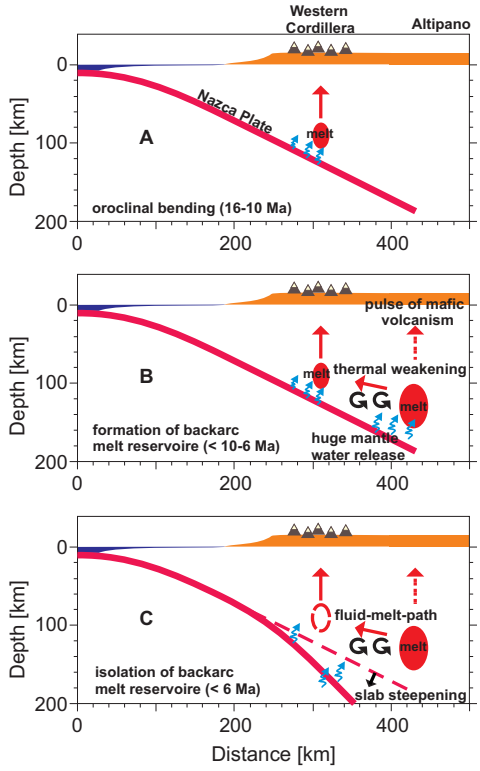

Figure 9: Attempt to reconstruct Neogene Nazca plate subduction in the Bolivian orocline:

A) Increased hydration of oceanic Nazca plate mantle due to significant oroclinal bending.

B) 2-4 Ma later, highly hydrated mantle reaches dehydration depths of serpentine (100-180 km) where the released fluids trigger high-grade partial melting in the backarc. Backarc melts rise vertically as well as non-vertically to the arc via internal convections.

C) Slab steepens during dehydration. The voluminous backarc reservoir persists but is maintained by less fluids. Volcanic productivity decreases.

Tracing the regression line of shallow Wadati-Benioff events ($z < 100$ km) to greater depths, this line cuts the mantle conductor at dehydration depths of serpentine ($z = 180$ km), the most important hydrous mantle mineral which may bound huge amounts of water. Therefore backarc peridotitic melting may have been triggered just above the slab by enormous fluid influx whereby the slab was compacting and steepening slowly to its actual position (fig. 9). Today, the magma reservoir should be maintained by much less fluidal material and probably cools down.

This scenario implies a prior period of extensive oceanic mantle hydration which might have occured during phases of oroclinal bending. Bending dates are hard to fix, probably block rotations in the closer survey area give a hint, they were dated at 12 Ma (Wörner *et al.*, 2000).

Using an average for ancient subduction rates of 10 cm/a, evaluated by Somoza (1998), and a constant slab dip of 25°, those huge amounts of fixed water will have started to deliberate after 2.4 Ma of subduction ($z \approx 100$ km) and will have reached depths of high-grade partial backarc melting ($z \approx 180$ km) further 1.9 Ma later. Surficial expression of high-grade mantle melting are Pliocene to recent pulses of mafic andesites erupting in the Bolivian Altiplano backarc (Davidson & de Silva, 1994). Furthermore backarc mantle magma might have been transported via internal convections to the sub-arc region and have also erupted at the main volcanic arc. However, the basal input into the deep magma system of the recent strato-volcanoes is only minor (Wörner *et al.*, 2000).

Conclusion

The huge backarc mantle conductor imaged by 2-D inversion of magnetotelluric data from the central Bolivian orocline inspired reflections about fluid and melt dynamics in the central Andean subduction zone. Among the two approaches considered here to explain the remarkable offset between intermediate depths mircoseismic events and the imaged magma reservoir, sub-arc and -backarc water release plays a key role for subduction zone dynamics.

In the central Bolivian orocline huge amounts of water might have been released at main slab dehydration depths some million years after oroclinal bending occurred where faults should have opened not only parallel but also perpendicular to the trench allowing deep water infiltration and fixation in the oceanic mantle. This implies on the one hand that mantle viscosity is definitely lowered and leads to significant material transports due to thermal convections, whereby fluids and melts may be widespreaded in the arc and backarc mantle. On the other hand, enhanced slab dehydration and slab compacting may have been followed by slab steepening and the imaged mantle melting process isn't supplied by much fluidal material anymore and therefore probably cools down.

References

Allmendinger, R.W., Jordan, T.E., Kay, S.M., & Isacks, B.L. 1997. The evolution of the Altiplano-Puna plateau of the Central Andes. *Annual Review of Earth and Planetary Sciences*, **25**, 139–174.

ANCORP Working Group. 2003. Seismic imaging of a convergent continental margin and plateau in the Central Andes (ANCORP'96). *Journal of Geophysical Research*, **108 (B7)**, 2328, doi:10.1029/2002JB001771.

Beck, S.L., & Zandt, G. 2002. The nature of orogenic crust in the Central Andes. *Journal of Geophysical Research*, **107**(B10), doi:10.1029/2000JB000124.

Brasse, H., & Eydam, D. 2008a. Electrical conductivity beneath the Bolivian Orocline and its relation to subduction processes at the South American continental margin. *Journal of Geophysical Research*, **113**(B07109), doi:10.1029/2007JB005142.

Brasse, H., Lezaeta, P., Rath, V., Schwalenberg, K., Soyer, W., & Haak, V. 2002. The Bolivian Altiplano conductivity anomaly. *Journal of Geophysical Research*, **107**(B5), doi:10.1029/2001JB000391.

Brasse, H., Kapinos, G., Li, Y., Mütschard, L., Soyer, W., & Eydam, D. 2008b. Structural electrical anisotropy in the crust at the South-Central Chilean continental margin as inferred from geomagnetic transfer functions. *Physics of the Earth and Planetary Interiors*, **173**, 7–16.

Currie, C.A., & Hyndman, R.D. 2006. The thermal structure of subduction zone back arcs. *Journal of Geophysical Research*, **111**, doi:10.1029/2005JB004024.

David, C. 2007. *Comportement actuel de l'avant arc et de l'arc du coude de Arica dans l'orogénèse des Andes Centrales*. PhD thesis at university Toulouse III.

Davidson, J.P., & de Silva, S.L. 1994. Late Cenozoic magmatism of the Bolivian Altiplano. *Contributions to Mineralogy and Petrology*, **119 (4)**, 387–408.

Dorbath, C., & Granet, M. 1996. Local earthquake tomography of the Altiplano and the Eastern Cordillera of northern Bolivia. *Tectonophysics*, **259**, 117–136.

Elger, K., Oncken, O., & Glodny, J. 2005. Plateaustyle accumulation of deformation: Southern Altiplano. *Tectonics*, **24**, doi:10.1029/2004TC001675.

Engdahl, E.R., & Villaseñor, A. 2002. Global Seismicity: 1900-1999. In: Int. Handbook of Earthquake and Engineering Seismology, Part A (eds. Lee, W.H.K., Kanamori, H., Jennings, P.C. & Kisslinger, C.). Academic Press, 665–690.

Eydam, D. 2008. *Magnetotellurisches Abbild von Fluid- und Schmelzprozessen in Kruste und Mantel der zentralen Anden*. Diploma thesis at Freie Universität Berlin.

Gerya, T.V., Connolly, J.A.D., Yuen, D.A., Gorczyk, W., & Capel, A.M. 2006. Seismic implication of mantle wedge plumes. *Earth and Planetary Science Letters*, **156**, 59–74.

Grove, T. L., Chatterjee, N., Parman, S. W., & Médard, E. 2006. The influence of water on mantle wedge melting. *Earth and Planetary Science Letters*, **249**, 74–89.

Gutscher, M.-A., Spakman, W., Bijwaard, H., & Engdahl, E. R. 2000. Geodynamics of flat subduction: Seismicity and tomographic constraints from the Andean margin. *Tectonics*, **19**(5), 814–833.

Hoke, L., Hilton, D., Lamb, S., Hammerschmidt, K., & Friedrichsen, H. 1994. ^{3}He evidence for a wide zone of active mantle melting beneath the Central Andes. *Earth and Planetary Science Letters*, **128**, 341–355.

Hérail, G., Rochat, P., Baby, P., Aranibar, O., Lavenu, A., & Masclez, G. 1997. El Altiplano Norte de Bolivia, evolución geológica terciaria. In: El Altiplano: ciencia y conciencia en los Andes, Actas 2. Simposio Internacional Estudios Altiplánicos, Arica 1993. R. Charrier, P. Aceituno, M. Castro, A. Llanos and L.A. Raggi (eds). Universidad de Chile: Santiago. 33-44.

James, D.E., & Sacks, I.S. 1999. Cenozoic formation of the Central Andes: A geophysical perspective. *Society of Economic Geology, Special Publication*, **7**, 1–26.

Klotz, J., Abolghasem, A., Khazaradze, G., Heinze, B., Vietor, T., Hackney, R., Bataille, K., Maturana, R., Viramonte, J., & Perdomo, R. 2006. Long-term signals in the present-day deformation field of the central and southern Andes and constraints on the viscosity of the earths upper mantle. In: The Andes: Active Subduction Orogeny. O. Oncken et al. (Eds.). Berlin: Springer. 65–89.

Kurtz, R.D., Delaurier, J.M., & Gupta, J.C. 1986. A magnetotelluric sounding across Vancouver Island detects the subducting Juan de Fuca plate. *Nature*, **321**, 596–599.

Lamb, S., & Davis, P. 2003. Cenozoic climate change as a possible cause for the rise of the Andes. *Nature*, **425**, 792–797.

Lezaeta, P. 2001. *Distortion analysis and 3-D modeling of magnetotelluric data in the Southern Central Andes*. PhD thesis at Freie Universität Berlin.

Mibe, K., Fujii, T., & Yasuda, A. 1999. Control of the location of the volcanic front in island arcs by aquous fluid connectivity in the mantle wedge. *Nature*, **401**, 259–262.

Muñoz, N., & Charrier, R. 1996. Uplift of the western border of the Altiplano on a west-vergent thrust system, Northern Chile. *Journal of South American Earth Sciences*, **9**, 171–181.

Ranero, C.R., & Sallarès, V. 2004. Geophysical evidence for alteration of the crust and mantle of the Nazca Plate during bending at the North Chile trench. *Geology*, **32**(2), 549–552.

Rodi, W., & Mackie, R.L. 2001. Nonlinear conjugate gradients algorithm for 2-D magnetotelluric inversions. *Geophysics*, **66**, 174–187.

Rüpke, L.H., Morgan, J.P., Hort, M., & Connolly, J.A.D. 2004. Serpentine and the subduction zone water cycle. *Earth and Planetary Science Letters*, **223**, 17–34.

Scambelluri, M., & Philippot, P. 2001. Deep fluids in subduction zones. *Lithos*, **55**, 213–227.

Scheuber, E., Bogdanic, T., Jensen, A., & Reutter, K.J. 1994. Tectonic development of the North Chilean Andes in relation to plate convergence and magmatism since the Jurassic. In: Tectonics of the Southern Central Andes. K.J. Reutter, E. Scheuber and P.J. Wigger (eds). Berlin: Springer. 121–139.

Schwarz, G., & Krüger, D. 1997. Resistivity cross section through the southern Central Andes as inferred from magnetotelluric and geomagnetic deep soundings. *Journal of Geophysical Research*, **102**, 11957–11978.

Sempere, T., Hérail, G., Oller, J., & Bonhomme, J. 1990. Late Oligocene - early Miocene major tectonic crisis and related basins in Bolivia. *Geology*, **18**, 946–949.

Somoza, R. 1998. Updated Nazca (Farallon)-South America relative motions during the last 40 My: Implications for the mountain building in the central Andean region. *Journal of South American Earth Sciences*, **11**(3), 211–215.

Springer, M.H., & Förster, A. 1998. Heatflow density across the Central Andean subduction zone. *Tectonophysics*, **291**, 123–139.

Tassara, A., Götze, H.J., Schmidt, S., & Hackney, R. 2006. Three-dimensional density model of the Nazca plate and the Andean continental margin. *Journal of Geophysical Research*, **111**(B6), doi:10.1029/2005JB003976.

Varentsov, I.M., Golubev, N.G., Gordienko, V.V., & Sokolova, E.Y. 1996. Study of deep geoelectrical structure along EMSLAB Lincoln-Line. *Phys. Solid Earth*, **32**, 375–393.

von Huene, R., Weinrebe, W., & Heeren, F. 1999. Subduction erosion along the North Chile margin. *Journal of Geodynamics*, **27**, 345–358.

Wannamaker, P.E., Booker, J.R., Jones, A.G., Chave, A.D., Filloux, J.H., Waff, H.S., & Law, L.K. 1989. Resistivity cross-section through the Juan de Fuca subduction system and its tectonic implications. *Journal of Geophysical Research*, **94**, 14127–14144.

Whitman, D., Isacks, B.L., & Kay, S.M. 1996. Lithospheric structure and along-strike segmentation of the Central Andean Plateau: seismic Q, magmatism, flexure, topography and tectonics. *Tectonophysics*, **259**, 29–40.

Wigger, P.J., Schmitz, M., Araneda, M., Asch, G., Baldzuhn, S., Giese, P., Heinsohn, W.D., Martinez, E., Ricaldi, E., Röwer, P., & Viramonte, J. 1994. Variation in the crustal structure of the Southern Central Andes deduced from seismic refraction investigations. In: Tectonics of the Southern Central Andes. K. J. Reutter and E. Scheuber and P. J. Wigger (eds). Berlin: Springer. 23–48.

Wörner, G., Uhlig, D., Kohler, I., & Seyfried, H. 2002. Evolution of the West Andean Escarpment at 18° S (N. Chile) during the last 25 Ma: Uplift, erosion and collapse through time. *Tectonophysics*, **345**, 183–198.

Wörner, G., López-Escobar, L., Moorbath, S., Horn, S., Entenmann, J., & Davidson, J.D. 1992. Variaciones geoquímicas, locales y regionales, en el arco volcánico Andino del norte de Chile (17°30'S-22°00'S). *Revista Geológica de Chile*, **19**(1), 37–56.

Wörner, G., Hammerschmidt, K., Henjes-Kunst, F., Lezaun, J., & Wilke, H. 2000. Geochronology (^{40}Ar/^{39}Ar, K-Ar and He-exposure ages) of Cenozoic magmatic rocks from Northern Chile (18-22°S): Implications for magmatism and tectonic evolution of the Central Andes. *Revista Geológica de Chile*, **27**, 205–240.